

PAPER

[View Article Online](#)
[View Journal](#) | [View Issue](#)Cite this: *Dalton Trans.*, 2022, **51**, 8906Heterometathesis of diphosphanes (R_2P-PR_2) with dichalcogenides ($R'E-ER'$, $E = O, S, Se, Te$)†Callum Branfoot,^a Paul G. Pringle,^a Natalie E. Pridmore,^a Tom A. Young^b and Duncan F. Wass^c

The reactions of R_2P-PR_2 with $R'E-ER'$, (where $E = Se, S, O, Te$) to give R_2P-ER' have been explored experimentally and computationally. The reaction of Ph_2P-PPh_2 with $PhSe-SePh$ gives $Ph_2P-SePh$ (**1**) rapidly and quantitatively. The $P-P/Se-Se$ reaction is inhibited by the addition of the radical scavenger TEMPO which is consistent with a radical mechanism for the heterometathesis reaction. Compound **1** has been fully characterised, including by X-ray crystallography. A range of other Ar_2P-SeR ($R = Ph, ^tBu$ or $CH_2CH_2CO_2H$) have also been prepared and characterised. The reaction of **1** with $[Mo(CO)_4(nbd)]$ ($nbd =$ norbornadiene) gives two products which, from their characteristic ^{31}P NMR data, have been identified as *cis*- $[Mo(CO)_4(Ph_2PSePh-P)_2]$ (**8**) and the mixed-donor complex *cis*- $[Mo(CO)_4(Ph_2P-SePh-P)(Ph_2P-SePh-Se)]$ (**9**). It is deduced that the P and Se atoms in ligand **1** have comparable capacity to coordinate to Mo(0). The reaction of Ph_2P-PPh_2 with $PhS-SPh$ gives Ph_2P-SPh (**2**) quantitatively but no reaction was observed between Ph_2P-PPh_2 and $PhTe-TePh$. Heterometathesis between Ph_2P-PPh_2 and $^tBuO-O^tBu$ does not occur thermally but has been observed under UV irradiation to give Ph_2P-O^tBu along with P(V) oxidation by-products. DFT calculations have been carried out to illuminate why heterometatheses with dichalcogenides $R'E-ER'$ occur readily when $E = S$ and Se but not when $E = O$ and Te . The calculations show that heterometathesis is predicted to be thermodynamically favourable for $E = O, S$ and Se and unfavourable for $E = Te$. The fact that a metathesis reaction between Ph_2P-PPh_2 with $^tBuO-O^tBu$ is not observed in the absence of UV radiation, is therefore due to kinetics.

Received 8th April 2022,
Accepted 19th May 2022

DOI: 10.1039/d2dt01093c

rsc.li/dalton

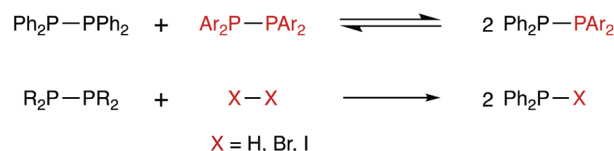
Introduction

The chemistry of diphosphanes (R_2P-PR_2) has attracted considerable attention, and the high reactivity of the P-P bond has been exploited for the diphosphination of a wide range of unsaturated substrates, including alkenes,^{1–4} alkynes,^{4–8} 1,3-dienes,⁹ arynes,¹⁰ CO_2 and CS_2 .¹¹ We recently reported that tetra-aryldiphosphanes readily undergo homometathesis reactions (Scheme 1) under ambient conditions, most likely *via* homolysis of the P-P bond and the generation of Ar_2P^\bullet radicals.¹² Also shown in Scheme 1 are diphosphane reactions with diatomic X_2 that could be classed as examples of diphosphane heterometathesis reactions.^{13,14}

Here, we report our experimental and computational investigations of the heterometatheses shown in Scheme 2¹⁵

and show that this is an effective route for the synthesis of compounds of the type Ph_2P-SeR .

Compounds containing P-S or P-Se bonds have been widely applied in organic synthesis as reagents for S or Se transfer (Lawesson's reagent¹⁶ and Woollins' reagent¹⁷ respectively). Furthermore, P/S and P/Se compounds are of interest in their own right^{18–20} with potential applications ranging from semi-conductors to pesticides.²¹ However, to date, little attention has been given to compounds of the type R_2P-SR or R_2P-SeR which are amongst the simplest organophosphorus(III) compounds containing S or Se. Arbuzov reported the first examples of Ph_2P-SR ($R =$ alkyl) compounds over a century ago.²² In the 1960s, McLean reported the synthesis of $Ph_2P-SePh$ (**1**) and Ph_2P-SPh (**2**) from Ph_2PCl by the routes shown in



Scheme 1 Metathesis reactions of diphosphanes.

^aSchool of Chemistry, University of Bristol, Cantock's Close, Bristol BS8 1TS, UK.
E-mail: paul.pringle@bristol.ac.uk^bChemistry Research Laboratory, University of Oxford, Oxford OX1 3TA, UK^cCardiff Catalysis Institute, School of Chemistry, Cardiff University, Cardiff CF10 3AT, UK† Electronic supplementary information (ESI) available. CCDC 2162103. For ESI and crystallographic data in CIF or other electronic format see DOI: <https://doi.org/10.1039/d2dt01093c>



Scheme 2

Scheme 3 Previously reported $\text{Ar}_2\text{P}-\text{ER}$ compounds.^{23,24}

Scheme 3, although no NMR spectroscopic data for these compounds were reported.²³ More recently, Cui *et al.*²⁴ prepared thioaniline derivative **3** similarly (Scheme 3).

Results and discussion

Diphosphane–diselenide metathesis

The reaction between equimolar quantities of tetraphenyldiphosphane and diphenyldiselenide in THF (Scheme 4) was monitored by $^{31}\text{P}\{^1\text{H}\}$ NMR spectroscopy. After 10 min, the signal for $\text{Ph}_2\text{P}-\text{PPh}_2$ at $\delta(\text{P}) -15.0$ ppm had been replaced by a singlet at $\delta(\text{P}) +29.4$ ppm with ^{77}Se satellites ($^1J_{\text{PSe}} = 229$ Hz); the $^{77}\text{Se}\{^1\text{H}\}$ NMR spectrum is a doublet at $\delta(\text{Se}) 307.5$ ppm ($^1J_{\text{PSe}} = 229$ Hz), consistent with the formation of the selanylphosphane, $\text{Ph}_2\text{P}-\text{SePh}$ (**1**). The product was isolated in 92% yield and further characterised by ^1H and $^{13}\text{C}\{^1\text{H}\}$ NMR, and

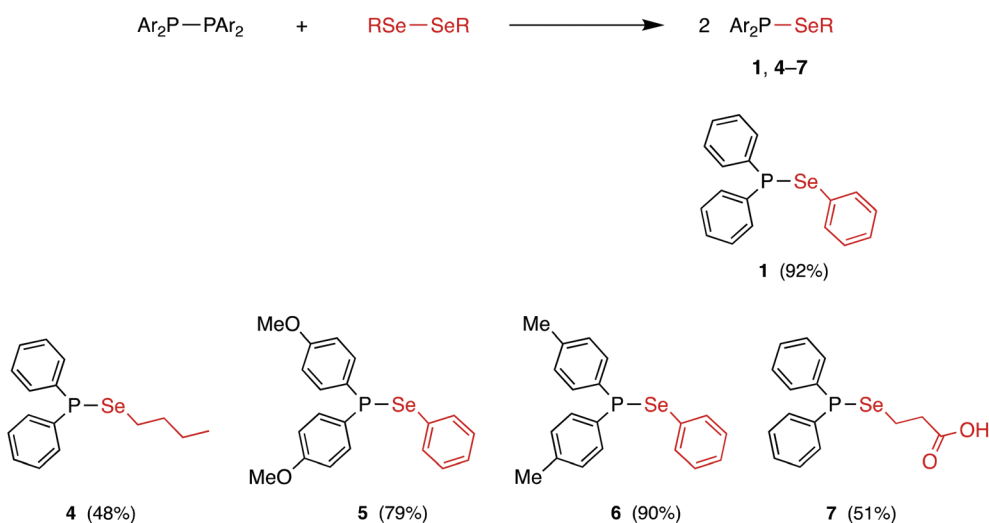
mass spectrometry (see ESI† for the data).²⁵ Crystals of **1** were grown from $\text{CH}_2\text{Cl}_2/n$ -hexane *via* vapour diffusion and its X-ray crystal structure determined (see Fig. 1).

The P–Se bond length in **1** of 2.2620(5) Å is close to the mean average of 2.217 Å obtained from the 686 single crystal X-ray structures that feature a P–Se bond in the Cambridge Structural Database (CSD). There are no crystal structures in the CSD of compounds of the type $\text{Ar}_2\text{P}-\text{SeAr}'$ (or $\text{Ar}_2\text{P}-\text{SAr}'$) with which to compare **1**, but the pyramidal geometry at P and bent geometry at Se are as expected.

The $\text{P}_2\text{R}_4/\text{Se}_2\text{R}_2$ heterometathesis reaction has been extended to the preparation of the new selanylphosphanes **4–7** (Scheme 4) by combination of the appropriate diphosphane and diselenide. Each of these compounds was isolated in good yield (quantitative yields observed by *in situ* $^{31}\text{P}\{^1\text{H}\}$ NMR spectroscopy) as an oil or oily solid and then fully characterised by $^{31}\text{P}\{^1\text{H}\}$, $^{77}\text{Se}\{^1\text{H}\}$, ^1H , $^{13}\text{C}\{^1\text{H}\}$ and APCI mass spectrometry (see ESI† for the data). The modest isolated yields of **4** and **7**



Fig. 1 Thermal ellipsoid (50% probability) representation of the crystal structure of diphenyl(phenylselanyl)phosphane (**1**), hydrogen atoms omitted for clarity. Selected bond lengths (Å) and bond angles (°): P1–Se1 2.2620(5), P1–C7 1.8421(18), P1–C13 1.8343(18), Se1–C1 1.9316(18); C7–P1–Se1 103.62(6), C7–P1–C13 100.15(8), C13–P1–Se1 96.38(6), P1–Se1–C1 98.66(5).



Scheme 4



(shown in Scheme 4) are due to losses during work-up, since the NMR yields were quantitative. These reactions were carried out in THF, CH_2Cl_2 or toluene and in no case was the solvent observed to affect the rate or outcome of the reaction, which in all cases had proceeded to completion within the time required (*ca.* 30 s) to obtain a $^{31}\text{P}\{^1\text{H}\}$ NMR spectrum of the reaction mixture. Of particular note is the carboxylic acid **7**, which shows that the P–Se bond is tolerant of reactive functional groups. The synthesis of **1** in CDCl_3 was repeated in an amberised NMR tube (to reduce the effect of photolysis) but again, complete conversion to **1** was observed within 30 s.

When the reaction of $\text{Ph}_2\text{P}-\text{PPh}_2$ with $\text{PhSe}-\text{SePh}$ was carried out in the presence of 4 equiv. of TEMPO in THF, the heterometathesis reaction was inhibited: in the absence of TEMPO, complete conversion was observed within 1 min, while in the presence of TEMPO, the reaction proceeded to 54% conversion after 90 min. Other products are detected associated with the formation of $\text{Ph}_2\text{P}-\text{TEMPO}$ species (see ESI†). This is consistent with radicals being involved in the reaction, as we previously demonstrated in the homometathesis of diphosphanes.¹² As a result, the radical chain mechanism shown in Scheme 5 is proposed. Diselenides are well-known to form RSe^\bullet radicals by photolytic cleavage of the weak Se–Se bond ($\text{BDE } 41 \text{ kcal mol}^{-1}$).^{26–32} It is therefore plausible that $\text{RSe}-\text{SeR}$ cleavage to produce RSe^\bullet radicals initiates the radical chain process shown in Scheme 5.³³

McLean reported²³ that $\text{Ph}_2\text{P}-\text{SePh}$ (**1**) is unstable with respect to isomerisation to $\text{Ph}_3\text{P}=\text{Se}$ at 100°C , over a period of 3–4 h. We have found that **1** is relatively stable under ambient conditions, which makes it easy to handle. Thus solid samples of **1** can be stored under argon at room temperature with <10% degradation observed (traces of Ph_2PH detected) even after 4 months. When water was added to a solution of **1**

in CDCl_3 and the emulsion shaken under nitrogen, only very slow hydrolysis to $\text{Ph}_2\text{P}(\text{O})\text{H}$ was observed: after 2 days, the hydrolysis mixture contained unreacted **1** (*ca.* 60%) along with a prominent signal (22%) at +32.5 ppm, consistent with the formation of $\text{Ph}_2\text{P}(\text{O})\text{OH}$;³⁴ crystals that grew from this solution were shown to match the structure of $\text{Ph}_2\text{P}(\text{O})\text{OH}$, ‘DPPHIN’ in the CSD.

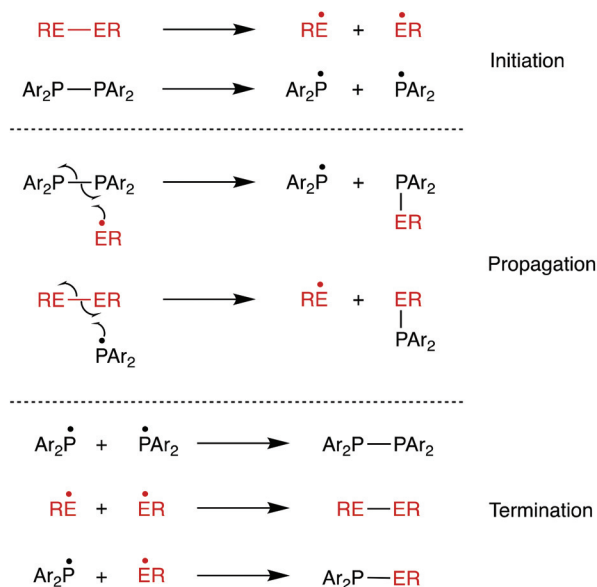
The observed kinetic stability of selanylphosphane **1** prompted us to explore its coordination chemistry with $\text{Mo}(0)$. To the best of our knowledge, selanylphosphanes have not previously been used as ligands for transition metals. It was of interest to investigate which of the two potential donor atoms (P and Se) would bind to the metal in the complexes, since both are known to bind to metals in mixed P,Se ligands such as $\text{Ph}_2\text{PCH}_2\text{CH}_2\text{SePh}$.^{35–37} Treatment of $[\text{Mo}(\text{CO})_4(\text{nbd})]$ (nbd = norbornadiene) with 2 equiv. of **1** in CD_2Cl_2 , gave a mixture of two products in the ratio of *ca.* 4 : 1 according to $^{31}\text{P}\{^1\text{H}\}$ NMR spectroscopy (see Fig. 2), which have been assigned to the isomers of *cis*- $[\text{Mo}(\text{CO})_4(\text{1})_2]$ (**8** and **9** in Scheme 6) on the basis of their characteristic ^{31}P NMR parameters.

The major product is a singlet at $\delta(\text{P}) +59.7$ ppm with outer ^{77}Se satellites ($^1J_{\text{PSe}} = 333$ Hz) that are themselves split into doublets ($^2J_{\text{PP}} = 25$ Hz) and inner ^{77}Se satellites ($^3J_{\text{PSe}} = 40$ Hz). This product is assigned the structure **8** where both ligands are P-bound *cis* on the Mo; this is supported by the large coordination chemical shift ($\Delta\delta_{\text{P}} = +29.2$) and the small $^2J_{\text{PP}}$. The inequivalence observed in the satellites is a result of the loss of symmetry in the ^{77}Se isotopologue (see Fig. 2).

The second product is assigned structure **9**, containing one P-bound and one Se-bound ligand **1**, on the basis of the ^{31}P NMR data. Two doublets are observed at $\delta(\text{P}^1) +62.4$ ppm and $\delta(\text{P}^2) +17.8$ ppm ($^3J_{\text{PP}} = 22$ Hz). The $\Delta\delta_{\text{P}}$ of +31.2 for P^1 in **9** is similar to the $\Delta\delta_{\text{P}}$ of the P in **8** and is therefore consistent with P^1 being directly bound to Mo. The $\Delta\delta_{\text{P}}$ of –12.7 ppm for P^2 is assigned to the Se-bound ligand in **9**. After the mixture of products was heated to 60°C in CDCl_3 for 3.5 h, complex **9** was the dominant species (ratio of complexes **9** : **8** was 5 : 1 according to ^{31}P NMR spectroscopy, see ESI†). In the IR spectrum of the mixtures of **8** and **9**, several absorptions in the range $1892\text{--}2027 \text{ cm}^{-1}$ were evident, as expected for the $\nu(\text{CO})$ bands for these *cis* complexes present. Solutions of the molybdenum complexes **8** and **9** in a $\text{CH}_2\text{Cl}_2/\text{water}$ emulsion did not undergo any changes after 17 h, indicating good water tolerance.

The analogous complexation reaction of selanylphosphane **7** with $[\text{Mo}(\text{CO})_4(\text{nbd})]$ in CH_2Cl_2 produced a similar pattern of products according to ^{31}P NMR spectroscopy (see ESI†): two products in the ratio 4 : 1, with a singlet at +50.8 ppm (with ^{77}Se satellites) and two doublets at +54.0 and 17.7 ppm ($^3J_{\text{PP}} = 21$ Hz) consistent with the formation of analogues of **8** and **9**.

The notable conclusion from the Mo coordination chemistry is that, for $\text{Ph}_2\text{P}-\text{SeR}$, the PPh_2 and SeR groups have comparable donor ability. The fine balance between the linkage isomers with P or Se coordination is likely a consequence of the donor atoms both being soft and the steric hindrance around the SeR being less than around the PPh_2 .



Scheme 5 Radical chain mechanism proposed for diphosphane–dichalcogenide metathesis.



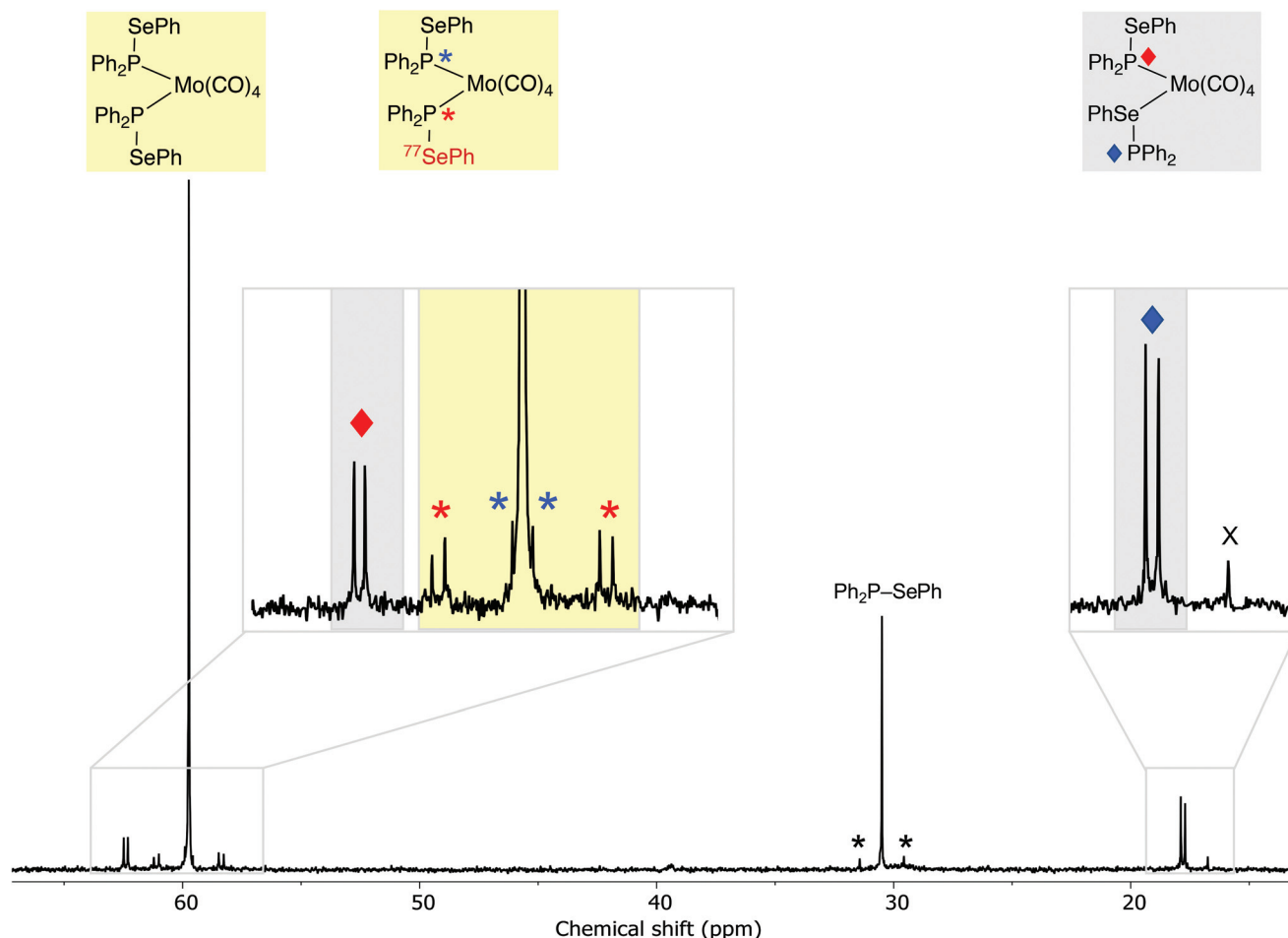
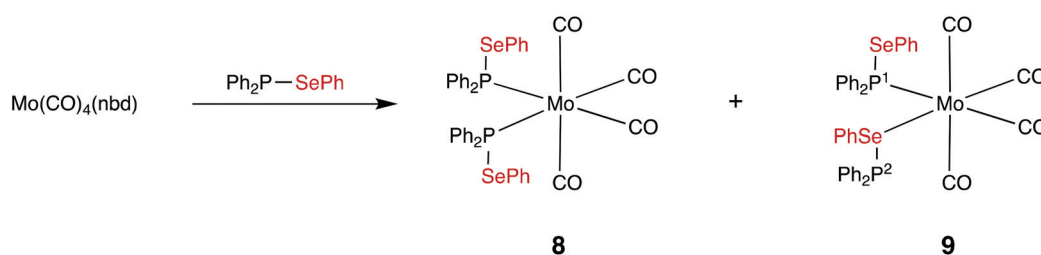


Fig. 2 $^{31}\text{P}\{^1\text{H}\}$ NMR spectrum of the product mixture obtained from the reaction of $\text{Ph}_2\text{P}-\text{SePh}$ with $[\text{Mo}(\text{CO})_4(\text{nbd})]$. The large singlet at ca. 60 ppm is assigned to the symmetrical P,P-complex **8** and the expansion shows the signals associated with the ^{77}Se isotopologue of **8**, which show satellite signals due to $^1J_{\text{PSe}}$ (*) and $^3J_{\text{PSe}}$ (*). The doublets at ca. +62 (♦) and +18 (♦) are assigned to **9**, the P,Se-linkage isomer of **8** (^{77}Se satellites obscured by the noise). The signal at ca. 31 ppm is for unreacted ligand **1** with ^{77}Se satellites (*). The minor signal labelled X at ca. +17 ppm is unassigned.



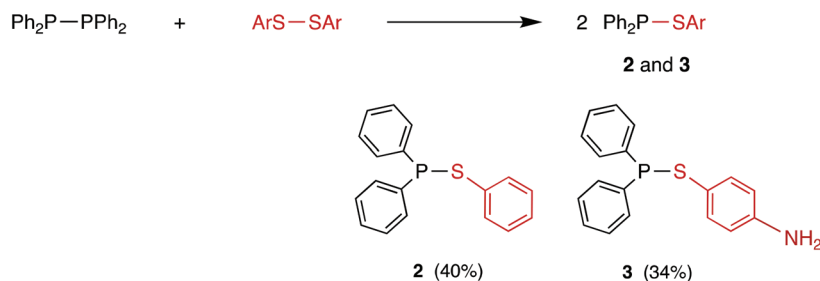
Scheme 6

Diphosphane–disulfide metathesis

The reaction of tetraphenyldiphosphane with diphenyl disulfide or 4-aminophenyl disulfide gave the previously reported sulfanyldiphosphanes **2** and **3** respectively (see Scheme 7).^{23,24,38} Compared with the rapid diselenide reactions (Scheme 4), the disulfide analogues are sluggish, requir-

ing up to 20 h to reach completion in an unagitated NMR tube. The reactions were significantly more rapid when they were stirred and were most rapid in chloroform (as with the diphosphane homometathesis).¹² The conversions to **2** and **3** were apparently quantitative in the reactions monitored by $^{31}\text{P}\{^1\text{H}\}$ NMR spectroscopy but the isolated yields were modest (see Scheme 7); there were significant losses on the





Scheme 7

short alumina column used to purify the crude products (see ESI†).

The diphosphane–disulfide metathesis was inhibited by the presence of TEMPO (4 equiv.), consistent with the reaction following the radical chain mechanism shown in Scheme 5, as for the diphosphane–diselenide process. The reaction of $\text{Ph}_2\text{P}-\text{PPh}_2$ with $\text{PhS}-\text{SPh}$ in CDCl_3 was followed by $^{31}\text{P}\{^1\text{H}\}$ NMR spectroscopy and **2** was formed in 34% yield after 1 h of reaction. When the same reaction was performed in the presence of 4 equivalents of TEMPO, 8% conversion to **2** was observed after 1 h (see ESI†). The higher rate observed with the diselenide than with the disulfide reflects the ease with which homolysis of the weak Se–Se bond takes place compared to the homolysis of either the S–S or P–P bonds.^{39–41}

Attempted diphosphane–ditelluride and diphosphane–peroxide metatheses

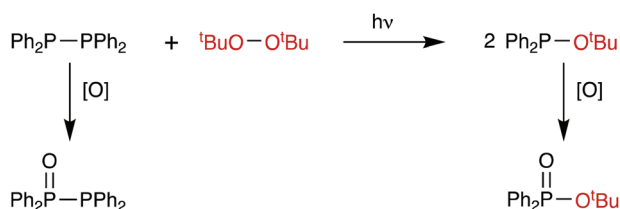
When $\text{Ph}_2\text{P}-\text{PPh}_2$ and $\text{PhTe}-\text{TePh}$ were mixed in C_6D_6 , no heterometathesis reaction (Scheme 2) was observed even after 12 days. The compound $\text{Ph}_2\text{P}-\text{TePh}$ has not been previously reported, although its P(v) isomer $\text{Ph}_3\text{P}=\text{Te}$ is readily prepared.⁴²

Similarly, when $\text{Ph}_2\text{P}-\text{PPh}_2$ and $t\text{BuO}-\text{O}t\text{Bu}$ were mixed in toluene, no heterometathesis reaction (Scheme 8) to give the known¹⁷ compound $\text{Ph}_2\text{P}-\text{O}t\text{Bu}$ was observed after 72 h. The only products detected by $^{31}\text{P}\{^1\text{H}\}$ NMR spectroscopy were the monoxide $\text{Ph}_2\text{P}(\text{O})-\text{PPh}_2$ (12%: 2 doublets at +32.7 and –24.7, $J_{\text{PP}} = 218 \text{ Hz}$)⁴³ and Ph_2PH (12%, –40.2 ppm).¹² Even when a large excess (~15-fold) of $t\text{BuO}-\text{O}t\text{Bu}$ was used and the reaction mixture was heated to 60 °C, only oxidation products were observed and no heterometathesis product. However, when this reaction was repeated in C_6D_6 and irradiated with near-UV

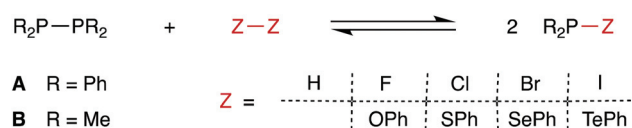
light, gradual formation of a new species was observed by $^{31}\text{P}\{^1\text{H}\}$ NMR spectroscopy characterised by a singlet at +87.1 ppm and assigned to the phosphinite $\text{Ph}_2\text{P}-\text{O}t\text{Bu}$ on the basis of the chemical shift being consistent with the reported value.⁴⁴ After the irradiation was continued for a further 1 h, a significant quantity of the phosphinate $\text{Ph}_2\text{P}(\text{O})-\text{O}t\text{Bu}$ (47% of the total ^{31}P integral, see ESI†) was identified by a singlet at +25.7 ppm, in good agreement with literature data.⁴⁵ The formation of this P(v) species was further supported by the detection of the phosphinate $[\text{M} + \text{Na}]^+$ ion by mass spectrometry (297.1 m/z observed, 297.1 theoretical). In summary, there is evidence that under UV irradiation, the diphosphane/peroxide heterometathesis does indeed occur but that by-products associated with oxidation by $t\text{BuO}-\text{O}t\text{Bu}$ contaminate the product (see Scheme 8).

DFT study of heterometathesis reactions of diphosphanes

The general reaction that has been calculated is shown in Scheme 9 and the results are given in Table 1. It was anticipated that the results for the diphosphane metatheses with diatomic molecules Z_2 would be the simplest to interpret. The DFT-calculated ΔE values for the addition of diatomic Z_2 to $\text{R}_2\text{P}-\text{PR}_2$, where $\text{R} = \text{Ph}$ (A), or Me (B), are presented as entries 1–10 of Table 1. The values of ΔH estimated using the mean bond strengths for P–P (51 kcal mol^{–1}),⁴⁶ Z–Z, and P–Z are also given in Table 1 and there is good agreement between ΔE and ΔH for $\text{Z} = \text{H}, \text{F}, \text{Cl}, \text{Br}$ and I . The two consistent trends in the heterometathesis equilibria are: (i) ΔE becomes increasingly more favourable with increasing electronegativity of Z ; (ii) $\text{Me}_2\text{P}-\text{PMe}_2$ metatheses are more favourable (by 6–10 kcal mol^{–1}) than the corresponding $\text{Ph}_2\text{P}-\text{PPh}_2$ metatheses. The position of the equilibrium in Scheme 9 is determined by the relative Z–Z and P–Z bond energies, which in turn will be influenced by a combination of the following factors. (a) The very high H–H and very low F–F bond strengths dominate the



Scheme 8



Scheme 9



Table 1 Calculated ΔE for the heterometatheses shown in Scheme 9^a

Entry	Diphosphane	Z-Z	$D(Z-Z)$	Product	$D(P-Z)$	ΔH	ΔE
1	A	H ₂	104	Ph ₂ P-H	77	+1	+6.8
2	A	F ₂	37	Ph ₂ P-F	117	-146	-131.2
3	A	Cl ₂	58	Ph ₂ P-Cl	79	-49	-44.1
4	A	Br ₂	45	Ph ₂ P-Br	65	-34	-28.9
5	A	I ₂	36	Ph ₂ P-I	51	-15	-10.9
6	B	H ₂	104	Me ₂ P-H	77	+1	+0.7
7	B	F ₂	37	Me ₂ P-F	117	-146	-141.3
8	B	Cl ₂	58	Me ₂ P-Cl	79	-49	-52.4
9	B	Br ₂	45	Me ₂ P-Br	65	-34	-36.6
10	B	I ₂	36	Me ₂ P-I	51	-15	-17.9
11	A	^t BuO-O ^t Bu	33	Ph ₂ P-O ^t Bu	84	-84	-69.4
12	A	PhO-OPh	33	Ph ₂ P-OPh	84	-84	-71.7
13	A	PhS-SPh	51	Ph ₂ P-SPh	55	-8	-4.2
14	A	PhSe-SePh	41	Ph ₂ P-SePh	—	—	-5.6
15	A	PhTe-TePh	—	Ph ₂ P-TePh	—	—	7.4

^a All energies are given in kcal mol⁻¹ and are calculated at STP (298 K, 1 atm). $D(Z-Z)$ and $D(P-Z)$ are the average bond dissociation energies given in ref. 46.

explanation of why the metathesis equilibria with H₂ and F₂ are the least and most favourable respectively. (b) The electrostatic stabilising effect of the P^{δ+}-Z^{δ-} dipole on the P-Z bond strength will increase with increasing electronegativity of Z. (c) The size of Z increases in the order F < Cl < Br < I and this will contribute to a lower P-Z bond strength (in that same order) due to increasingly poorer orbital overlap and increasing steric congestion. (d) The P-Z bond may be stronger in Me₂P-Z than in Ph₂P-Z, due to the lower steric hindrance of the PMe₂ group and the greater +I inductive effect of the Me substituents stabilising the δ+ charge on the PMe₂.⁴⁷

The calculated thermodynamics of the metathesis reactions of Ph₂P-PPh₂ with PhE-EPh, where E = O, S, Se, or Te are given in Table 1, entries 12–15. These equilibria will depend on the relative PhE-EPh and Ph₂P-EPh bond energies with potentially similar factors at play to those labelled (a)–(c) above, used for the diatomic Z₂ reactions. However, in the case of the dichalcogenides, the PhO-OPh equilibrium (entry 12) is exceptional in being extremely favourable (ΔE of -69.4 kcal mol⁻¹) as a consequence of the low O-O bond energy and the high P-O bond energy (due in part to the large P^{δ+}-Z^{δ-} dipole). By contrast, for the other dichalcogenides (entries 13–15), the ΔE values are relatively small, reflecting the fact that the P-P, E-E and P-E bond energies are similar due to the similarity of the electronegativities and sizes of P, S, Se and Te. The calculated ΔE for the diselenide and disulfide reactions are both *ca.* -5 kcal mol⁻¹ and therefore favour the formation of Ph₂P-EPh, in agreement with the experimental observations. The calculated ΔE of +7 kcal mol⁻¹ for the ditelluride/diphosphane metathesis disfavors the formation of Ph₂P-TePh which is consistent with no reaction between Ph₂P-PPh₂ and PhTe-TePh being observed experimentally.

Although the ^tBuO-O^tBu/Ph₂P-PPh₂ metathesis (entry 11, Table 1) is very strongly favoured energetically for the formation of Ph₂P-O^tBu, experimentally, the reaction (Scheme 8) only proceeded under UV irradiation and produced oxidation by-products; the lack of thermal reaction is therefore

due to a kinetic barrier, possibly caused by the bulky ^tBu substituents.

Conclusion

The heterometathesis reactions of Ph₂P-PPh₂ with RE-ER to give Ph₂P-ER proceed smoothly when E = S or Se but not when E = O or Te. We have shown that Ar₂P-PAr₂ with RSe-SeR gives a range of Ar₂P-SeR compounds (1 and 4–7) in quantitative spectroscopic yields and 100% atom-economy. The reaction of Ph₂P-PPh₂ with ArS-SAr produces Ph₂P-SAr, albeit more slowly than with the Se analogues. The inhibition by TEMPO of the heterometatheses of Ph₂P-PPh₂ with RE-ER (E = Se or S) suggests radical processes are involved in the mechanism. DFT calculations have shown that the heterometatheses with RE-ER are thermodynamically favourable when E = S or Se but not when E = Te, which aligns with the experimental observations. However, the calculations also suggest that the heterometathesis of diphosphanes with peroxides (*i.e.* E = O) would be very strongly favoured thermodynamically. The lack of thermal reaction between Ph₂P-PPh₂ with ^tBuO-O^tBu is therefore due to kinetics. There is evidence of formation of Ph₂P-O^tBu when mixtures of Ph₂P-PPh₂ and ^tBuO-O^tBu are photolysed but the reaction is complicated by the simultaneous formation of oxidation products. The selanylphosphane Ph₂P-SePh (1) can be stored for weeks, largely unchanged at ambient temperatures and is only very slowly hydrolysed by water over several days. The ligand properties of 1 are of interest as it coordinates to Mo(0) to give products whose ³¹P parameters are consistent with coordination *via* the P and Se being competitive. This is an unusual example of linkage isomerism that is worthy of further study.

Conflicts of interest

There are no conflicts to declare.



Acknowledgements

This research was funded by the Engineering and Physical Sciences Research Council through the EPSRC Centre for Doctoral Training in Advanced Composites for Innovation and Science (grant number EP/L0160208/1). We thank the Department of Chemistry at Oxford and the Centre for Computational Chemistry in Bristol for access to computing facilities.

References

- H. Yorimitsu, Homolytic substitution at phosphorus for C-P bond formation in organic synthesis, *Beilstein J. Org. Chem.*, 2013, **9**, 1269–1277.
- I. Hajdók, F. Lissner, M. Nieger, S. Strobel and D. Gudat, Diphosphination of Electron Poor Alkenes, *Organometallics*, 2009, **28**, 1644–1651.
- N. Otomura, Y. Okugawa, K. Hirano and M. Miura, Bromine Cation Initiated vic-Diphosphination of Styrenes with Diphosphines under Photoredox Catalysis, *Synthesis*, 2018, **50**, 3402–3407.
- K. Hirano and M. Miura, Recent advances in diphosphination of alkynes and alkenes, *Tetrahedron Lett.*, 2017, **58**, 4317–4322.
- D. L. Dodds, M. F. Haddow, A. G. Orpen, P. G. Pringle and G. Woodward, Stereospecific diphosphination of activated acetylenes: A general route to backbone-functionalized, chelating 1,2-diphosphinoethenes, *Organometallics*, 2006, **25**, 5937–5945.
- D. L. Dodds, J. Floure, M. Garland, M. F. Haddow, T. R. Leonard, C. L. McMullin, A. G. Orpen and P. G. Pringle, Diphosphanes derived from phobane and phosphatrioxa-adamantane: similarities, differences and anomalies, *Dalton Trans.*, 2011, **40**, 7137–7146.
- Y. Yamamoto, R. Tanaka, S. Kodama, A. Nomoto and A. Ogawa, Photoinduced Bisphosphination of Alkynes with Phosphorus Interelement Compounds and Its Application to Double-Bond Isomerization, *Molecules*, 2022, **27**, 1284.
- A. D. Gorman, J. A. Cross, R. A. Doyle, T. R. Leonard, P. G. Pringle and H. A. Sparkes, Phosphophosphidites Derived from BINOL, *Eur. J. Inorg. Chem.*, 2019, **2019**, 1633–1639.
- N. Otomura, K. Hirano and M. Miura, Diphosphination of 1,3-Dienes with Diphosphines under Visible-Light-Promoted Photoredox Catalysis, *Org. Lett.*, 2018, **20**, 7965–7968.
- Y. Okugawa, Y. Hayashi, S. Kawauchi, K. Hirano and M. Miura, Diphosphination of Alkynes with Diphosphines, *Org. Lett.*, 2018, **20**, 3670–3673.
- N. Szykiewicz, L. Ponikiewski and R. Grubba, Diphosphination of CO₂ and CS₂ mediated by frustrated Lewis pairs-catalytic route to phosphanyl derivatives of formic and dithioformic acid, *Chem. Commun.*, 2019, **55**, 2928–2931.
- C. Branfoot, T. A. Young, D. F. Wass and P. G. Pringle, Radical-initiated P,P-metathesis reactions of diphosphanes: evidence from experimental and computational studies, *Dalton Trans.*, 2021, **50**, 7094–7104.
- S. J. Geier and D. W. Stephan, Rh-catalyzed P-P bond activation, *Chem. Commun.*, 2008, **054**, 99–101.
- H. Hacklin and G.-V. Rösenthaller, 1-Halogenphosphorinane: Darstellung Und Derivate, *Phosphorus Sulfur Relat. Elem.*, 1988, **36**, 165–169.
- (a) The heterometathesis reaction between Ph₂Bi–BiPh₂ and PhE–EPh (E = S, Se, Te) to give Ph₂Bi–EPh has been previously reported, see: F. Calderazzo, A. Morvillo, G. Pelizzi, R. Poli and F. Ungari, Reactivity of Molecules Containing Element–Element Bonds. 1. Nontransition Elements, *Inorg. Chem.*, 1988, **27**, 3730–3733; (b) The reaction between Me₂P–PMe₂ and MeE–EME produces equilibrium mixtures with the corresponding Me₂P–EME (E = S, Se, Te); see: A. J. Ashe III and E. G. Ludwig Jr., The Exchange Reactions of Tetramethylpnictogens with Dimethyldichalcogenides, *J. Organomet. Chem.*, 1986, **308**, 289–296.
- T. Ozturk, E. Ertas and O. Mert, Use of Lawesson's reagent in organic syntheses, *Chem. Rev.*, 2007, **107**, 5210–5278.
- I. P. Gray, P. Bhattacharyya, A. M. Z. Slawin and J. D. Woollins, A New Synthesis of (PhPSe₂)₂ (Woollins Reagent) and Its Use in the Synthesis of Novel P–Se Heterocycles, *Chem. – Eur. J.*, 2005, **11**, 6221–6227.
- G. Hua, R. A. M. Randall, A. M. Z. Slawin and J. D. Woollins, Novel organo phosphorus-selenium heteroatom compounds from selenation of diamines, *Tetrahedron*, 2013, **69**, 5299–5305.
- L. Ascherl, A. Nordheider, K. S. A. Arachchige, D. B. Cordes, K. Karaghiosoff, M. Bühl, A. M. Z. Slawin and J. D. Woollins, The activation of Woollins' reagent. Isolation of pyridine stabilised PhPSe₂, *Chem. Commun.*, 2014, **50**, 6214–6216.
- G. Hua, Y. Li, A. M. Z. Slawin and J. D. Woollins, Unexpected four- and eight-membered organo P–Se heterocycles, *Chem. Commun.*, 2007, **83**, 1465–1467.
- R. Davies and L. Patel, in *Handbook of Chalcogen Chemistry: New Perspectives in Sulfur, Selenium and Tellurium*, ed. F. Devillanova and W.-W. Du Mont, Royal Society of Chemistry, 2nd edn, 2013, pp. 238–306.
- A. Arbuzov, *J. Russ. Phys.-Chem. Soc.*, 1910, **42**, 549.
- R. A. N. McLean, Phenylthio- and Phenylseleno-Diphenyl Phosphine, *Inorg. Nucl. Chem. Lett.*, 1969, **5**, 745–747.
- H. Cui, M. Hu, H. Wen, G. Chai, C. Ma, H. Chen and C. Chen, Efficient [FeFe] hydrogenase mimic dyads covalently linking to iridium photosensitizer for photocatalytic hydrogen evolution, *Dalton Trans.*, 2012, **41**, 13899–13907.
- P. J. Gates, Atmospheric pressure chemical ionisation mass spectrometry for the routine analysis of low molecular weight analytes, *Eur. J. Mass Spectrom.*, 2021, **27**, 13–28.
- R. Franzi and M. Geoffroy, Spin trapping identification of radical intermediates during photolysis of organoselenium compounds, *J. Organomet. Chem.*, 1981, **218**, 321–324.



- 27 T. G. Back and M. Vijaya Krishna, Free-Radical Additions of Diselenides to Dimethyl Acetylenedicarboxylate, Methyl Propiolate, and Dimethyl Maleate, *J. Org. Chem.*, 1988, **53**, 2533–2536.
- 28 D. H. Brown, R. J. Cross and D. Millington, Photochemical reactions between tertiary phosphines and organic diselenides, *J. Chem. Soc., Dalton Trans.*, 1977, 159–161.
- 29 M. M. Alam, O. Ito, Y. Koga and A. Ouchi, Laser-flash photolysis of naphthyl diselenides; reactivities of naphthylseleno radicals, *Int. J. Chem. Kinet.*, 1998, **30**, 193–200.
- 30 C. Liu, J. Xia, S. Ji, Z. Fan and H. Xu, Visible-light-induced metathesis reaction between diselenide and ditelluride, *Chem. Commun.*, 2019, **55**, 2813–2816.
- 31 J. Xia, S. Ji and H. Xu, Diselenide covalent chemistry at the interface: stabilizing an asymmetric diselenide-containing polymer via micelle formation, *Polym. Chem.*, 2016, **7**, 6708–6713.
- 32 S. Ji, W. Cao, Y. Yu and H. Xu, Dynamic diselenide bonds: exchange reaction induced by visible light without catalysis, *Angew. Chem., Int. Ed.*, 2014, **53**, 6781–6785.
- 33 The reaction of tetraphenyldiphosphane and dibenzyl diselenide gave the expected product $\text{Ph}_2\text{P}-\text{SeBn}$, identified by a singlet in the $^{31}\text{P}\{^1\text{H}\}$ NMR spectrum in CDCl_3 at +23.4 ppm, with ^{77}Se satellites ($J_{\text{PSe}} = 242$ Hz). However, after 25 min this resonance accounts for only 50% of the ^{31}P integral, with 37% residual tetraphenyldiphosphane and 13% formation of various other species (see ESI† for the spectrum). This contrasting reactivity is consistent with previous reports that photolysis of $\text{BnSe}-\text{SeBn}$ preferentially leads to cleavage of the C–Se bond, due to the relative stability of the benzyl radical. The mixture of BnSe^\bullet , Bn^\bullet , and BnSeSe^\bullet radicals present would explain the low conversion to $\text{Ph}_2\text{P}-\text{SeBn}$ and the formation of the by-products. See: E. N. Deryagina, M. G. Voronkov and N. A. Korchevin, Selenium- and tellurium-centred radicals, *Russ. Chem. Rev.*, 1993, **62**, 1107–1117.
- 34 J. Ash, H. Huang, P. Cordero and J. Y. Kang, Selective hydrolysis of phosphorus(V) compounds to form organophosphorus monoacids, *Org. Biomol. Chem.*, 2021, **19**, 6007–6014.
- 35 T. J. Cunningham, M. R. J. Elsegood, P. F. Kelly, M. B. Smith and P. M. Staniland, Versatile routes to selenoether functionalized tertiary phosphines, *Dalton Trans.*, 2010, **39**, 5216–5218.
- 36 A. M. Spokoyny, M. S. Rosen, P. A. Ulmann, C. Stern and C. A. Mirkin, Selective Formation of Heteroligated Pt(II) Complexes with Bidentate Phosphine-Thioether (P,S) and Phosphine-Selenoether (P,Se) Ligands via the Halide-Induced Ligand Rearrangement Reaction, *Inorg. Chem.*, 2010, **49**, 1577–1586.
- 37 M. S. Rosen, A. M. Spokoyny, C. W. Machan, C. Stern, A. Sarjeant and C. A. Mirkin, Chelating Effect as a Driving Force for the Selective Formation of Heteroligated Pt(II) Complexes with Bidentate Phosphino-Chalcoether Ligands, *Inorg. Chem.*, 2011, **50**, 1411–1419.
- 38 T. Shirai, S. Kawaguchi, A. Nomoto and A. Ogawa, Photoinduced highly selective thiophosphination of alkynes using a $(\text{PhS})_2/(\text{Ph}_2\text{P})_2$ binary system, *Tetrahedron Lett.*, 2008, **49**, 4043–4046.
- 39 D. Kaur, P. Sharma and P. V. Bharatam, A comparative study on the nature and strength of O–O, S–S, and Se–Se bond, *J. Mol. Struct.: THEOCHEM*, 2007, **810**, 31–37.
- 40 S. Kawaguchi and A. Ogawa, Applications of Diphosphines in Radical Reactions, *Asian J. Org. Chem.*, 2019, **8**, 1164–1173.
- 41 V. T. Hung, C. C. Tran, Y. Yamamoto, S. Kodama, A. Nomoto and A. Ogawa, Clarification on the reactivity of diaryl diselenides toward hexacyclohexyldilead under light, *Molecules*, 2021, **26**, 6265.
- 42 C. H. W. Jones and R. D. Sharma, ^{125}Te NMR And Mössbauer Spectroscopy of Tellurium-phosphine Complexes and the Tellurocyanates, *Organometallics*, 1987, **6**, 1419–1423.
- 43 M. S. Hill, M. F. Mahon and T. P. Robinson, Calcium-centred phosphine oxide reactivity: P–C metathesis, reduction and P–P coupling, *Chem. Commun.*, 2010, **46**, 2498–2500.
- 44 Y. Shinro, S. Kosei, Y. Masakuni, M. Toshihisa and O. Atsuyoshi, The Arbuzov Reaction of Alkyl Diphenylphosphinites with 10-Methylacridinium Ion. Kinetic Study on the Formation and the Decomposition of Phosphonium Intermediates, *Bull. Chem. Soc. Jpn.*, 1993, **66**, 2077–2083.
- 45 A. Kinbara, M. Ito, T. Abe and T. Yamagishi, Nickel-catalyzed C–P cross-coupling reactions of aryl iodides with H-phosphinates, *Tetrahedron*, 2015, **71**, 7614–7619.
- 46 C. Housecroft and A. G. Sharpe, *Inorganic Chemistry*, Pearson Education, 5th edn, 2018.
- 47 We previously proposed related electrostatic and steric contributions to rationalise the thermodynamics of homometathesis P–P equilibria, see ref. 12.

